Title
Resolving single cone inputs to visual receptive fields.

Journal
Nature neuroscience, 12(8)

ISSN
1097-6256

Authors
Sincich, Lawrence C
Zhang, Yuhua
Tiruveedhula, Pavan
et al.

Publication Date
2009-08-01

DOI
10.1038/nn.2352

Peer reviewed

Published in final edited form as:

Nat Neurosci. 2009 August ; 12(8): 967–969. doi:10.1038/nn.2352.

Resolving Single Cone Inputs to Visual Receptive Fields

Lawrence C. Sincich[1], **Yuhua Zhang**[2,3], **Pavan Tiruveedhula**[2], **Jonathan C. Horton**[1], and **Austin Roorda**[2]

[1]Beckman Vision Center, University of California, San Francisco, San Francisco, CA 94143

[2]School of Optometry, University of California, Berkeley, Berkeley, CA 94720

[3]Department of Ophthalmology, University of Alabama, Birmingham, AL 35233

Abstract

With current techniques for mapping receptive fields, it is impossible to resolve the contribution of single cone photoreceptors to the response of central visual neurons. Using adaptive optics to correct for ocular aberrations, we delivered micron-scale spots of light to the receptive field centers of neurons in the macaque lateral geniculate nucleus. Parvocellular LGN neurons mapped this way responded with high reliability to stimulation of single cones.

Keywords

photoreceptors; cone fields; lateral geniculate nucleus; color vision

Human vision is subserved by three types of cone photoreceptors, differing in spectral sensitivity, in density with respect to distance from the fovea, and in relative abundance across individuals1. Because the receptive field centers of most neurons in the early visual system are composed of multiple cones, the question arises whether the stimulation of just one cone is sufficient to activate retinal ganglion cells, and consequently for stimuli to be perceived. Moreover, given the dispersal of photoreceptor signals through the retinal layers2, it is likely that different cones will vary in their efficacy at driving downstream neural activity. Here we show that thalamic responses can be reliably mapped by stimulating individual cones, and that the probability of a evoking a spike with each stimulus flash varies, in part because of exquisite sensitivity to the position of stimuli relative to each cone.

Ordinarily, a neuron's response properties are characterized by presenting stimuli on a screen while recording action potentials with an extracellular electrode3. This yields a receptive field delimited in time and space, indicating what stimuli are effective at driving the cell. Such a method does not provide direct identification of the cones feeding the receptive field. This method is also limited by optical aberration, diffraction, scatter, pre-retinal absorption, and eye movement, which all degrade visual stimuli. These limitations

Corresponding author: Lawrence C. Sincich, PhD, Beckman Vision Center, University of California, San Francisco, Email: sincichl@vision.ucsf.edu, 10 Koret Way, San Francisco, CA 94143-0730, Phone: 415-476-8328, Fax: 415-476-0336.

alter the location and spectral intensity of light impinging on the photoreceptors, making it difficult to map the cone field precisely, especially near the fovea where cone spacing is only a few microns. To overcome these difficulties, we used an adaptive optics scanning laser ophthalmoscope (AOSLO) to visualize and stimulate directly the cones *in vivo* in the macaque4, 5 (details in Supplementary Methods online). Experiments were conducted using procedures approved by the UCSF Institutional Animal Care and Use Committee, in accordance with NIH guidelines. Neurons were recorded in the lateral geniculate nucleus (LGN), allowing us to explore receptive field properties that cannot be examined with traditional mapping techniques.

As expected from the retinotopic organization of the LGN, a orderly sequence of receptive fields was recorded in the left eye during one electrode penetration (Fig. 1a). Superimposed on the fundus photograph is a montage of AOSLO cone images (each 1.2° × 1.2°) used to aid navigation in the retina when searching for responsive cones. Once an LGN neuron was encountered, the first task was to find the retinal location where a flashed stimulus generated a response. We identified which cones produced the briskest firing by moving a flickering spot across the retina, a straightforward procedure because the cones being stimulated could be seen in real time (Supplementary Video 1 online).

The diameter of the cone field was then determined by plotting the neural response profile obtained by flashing a smaller stimulus pseudorandomly at locations spaced every 3 μm through the middle of the field (Fig. 1b). These 3 μm square stimuli subtended 52 arcsec, which is approximately equal to the diameter of one cone's inner segment at 3.7°, the eccentricity of this parvocellular ON-center field. Because the stimuli were constructed from a 30 Hz raster scan, the neural response was phase-locked to the frame rate, with the flash duration at each locus being about 5 μs (see Supplementary Fig. 1 online for details). Single stimulus flashes delivered to single cones led reliably to LGN spikes, with the likelihood of generating any spikes reaching 85% at the peak response location. Responses diminished sharply at the edge of the cone field, where a shift in the stimulus position of just 3 μm dropped the LGN spike probability to baseline, suggesting that light delivery was not affected seriously by optical blur or intraretinal scatter. Towards the limits of the tested area, the probability of firing began to dip below the baseline level, presumably reflecting inhibition from the receptive field surround.

The response profile of Neuron 1 (Fig. 1b) exhibits variation in spike probability at each stimulus location, particularly within the receptive field center. There are several possible sources for this variation. First, although parvocellular neurons are dominated by a single cone type, it is unclear if this property arises from only one cone type being wired up to the field center, or if one cone type simply outnumbers the others6–8. With the narrowband light used for stimulation (centered at 680 nm wavelength), *in vitro* measurements of macaque spectral sensitivities would predict that L-cones are 14 times more sensitive than M-cones, and 105.8 more so than S-cones9. However, the relationship between sensitivity differences and firing rate differences in downstream neurons is unclear, because neural responses often sum nonlinearly. Second, the synaptic weighting of the input from each cone to a ganglion cell, even from cones of the same type, may not be equal. Such variation in synaptic efficacy would be transmitted from ganglion cells to LGN neurons. Finally, a

significant source of variation could be the sensitivity of cones to the exact position of the stimulus, an effect heightened by their light-guide properties10.

To examine the sources of variability in more detail, it was crucial first to measure how well stimuli were restricted to single cones. As a direct test of the spatial impact of a stimulus spot, we recorded responses 6° from the fovea, where cones are more widely spaced. If intraretinal scatter were minimal and the AO-corrected spots were small enough, stimuli targeted between cones would be unlikely to drive responses effectively. Here we flashed rectangular stimuli that had a narrow dimension that was smaller than the gap between cones in the AO images (Fig. 2a). In this OFF-center cell, stimuli that impinged upon a single cone (positions 8 and 9) generated the largest response, while flanking stimuli that landed between cones (e.g. positions 7 and 10) evoked significantly fewer spikes. The response did not go to baseline at the flanks because the time-averaged energy distribution of the stimulus revealed that a fraction of light still landed on the adjacent cone profiles. As with other LGN neurons we recorded, some cones generated significantly different responses, even when stimuli were positioned over them in a similar fashion (e.g. responses at positions 8 and 14 in Fig. 2a; $p < 0.05$, one-tailed Fisher's exact test), implying that this neuron either received input from both L and M cones or had mixed cone weights. It is worth noting that cone-to-cone electrical coupling is present11, which will reduce the apparent discreteness of the stimuli actually delivered to the retina because coupled cones can funnel activity through single midget bipolar cells.

Variable response levels for different cones were found in all parvocellular LGN neurons ($n = 6$), and appeared more discrete when stimuli were kept small and positioned in small increments. The cone field for Neuron 3, a parvocellular ON-center cell (Fig. 2b), was probed with a 3 μm stimulus at twice the spatial resolution used for Neuron 1 (Fig. 1b). As the stimulus was shifted from cone to cone, the spike activity stepped to several distinct levels. The lowest response, which also exhibited a temporal delay, coincided with the extent of one cone, but was still above the background firing rate. This difference in spatiotemporal firing pattern suggests that an M cone was at this location, while the flanking higher responses probably originated from L cones. However, as mentioned earlier, it is also possible that color-tuned neurons are supplied by cones of the same type which differ in input strength. An instrument that allows stimulation with multiple wavelengths to facilitate direct assessment of the spectral tuning in each cone could address this issue.

Because LGN neurons respond reliably when only one of their cone inputs is stimulated, it suggests that single cone activation is sufficient for perception, even away from the fovea. This is supported by data showing that frequency-of-seeing curves asymptote well below 100% when small AO-corrected spots are flashed in a human subject missing a subpopulation of cones, because stimuli occasionally land in "holes" in the photoreceptor mosaic12. In normal subjects, frequency-of-seeing curves are also liable to be affected when such stimuli fall between cones13. With the ability to probe visual responses *in vivo* at their elemental level, the single cone, it will be possible to investigate how variable cone weighting leads to the deviations from cone "purity" seen for color-sensitive neurons in the LGN14 as well as primary visual cortex15.

Supplementary Material

Refer to Web version on PubMed Central for supplementary material.

Acknowledgments

We thank Q. Yang, D. W. Arathorn and M. Feusner for help with software development, and D. Williams and D. Copenhagen for insightful manuscript comments. This work was supported by National Eye Institute grants EY10217 (J.C.H.), EY014375 (A.R.) and EY02162 (Beckman Vision Center). Support was also received from the National Science Foundation, through grant IIS-0712852 (L.C.S.), the Center for Adaptive Optics cooperative agreement AST-9876783, managed by UC Santa Cruz, and Research to Prevent Blindness. The California Regional Primate Research Center is supported by NIH Base Grant RR00169.

References

1. Hofer H, Carroll J, Neitz J, Neitz M, Williams DR. Organization of the human trichromatic cone mosaic. J Neurosci. 2005; 25:9669–9679. [PubMed: 16237171]
2. Wassle H. Parallel processing in the mammalian retina. Nat Rev Neurosci. 2004; 5:747–757. [PubMed: 15378035]
3. Hubel DH, Wiesel TN. Receptive fields, binocular interaction and functional architecture in the cat's visual cortex. J Physiol. 1962; 160:106–154. [PubMed: 14449617]
4. Roorda A, et al. Adaptive optics scanning laser ophthalmoscopy. Optics Express. 2002; 10:405–412. [PubMed: 19436374]
5. Arathorn DW, et al. Retinally stabilized cone-targeted stimulus delivery. Optics Express. 2007; 15:13731–13744. [PubMed: 19550644]
6. Wiesel TN, Hubel DH. Spatial and chromatic interactions in the lateral geniculate body of the rhesus monkey. J Neurophysiol. 1966; 29:1115–1156. [PubMed: 4961644]
7. Diller L, et al. L and M cone contributions to the midget and parasol ganglion cell receptive fields of macaque monkey retina. J Neurosci. 2004; 24:1079–1088. [PubMed: 14762126]
8. Buzas P, Blessing EM, Szmajda BA, Martin PR. Specificity of M and L cone inputs to receptive fields in the parvocellular pathway: random wiring with functional bias. J Neurosci. 2006; 26:11148–11161. [PubMed: 17065455]
9. Baylor DA, Nunn BJ, Schnapf JL. Spectral sensitivity of cones of the monkey Macaca fascicularis. J Physiol. 1987; 390:145–160. [PubMed: 3443931]
10. Roorda A, Williams DR. Optical fiber properties of individual human cones. J Vis. 2002; 2:404–412. [PubMed: 12678654]
11. Hornstein EP, Verweij J, Schnapf JL. Electrical coupling between red and green cones in primate retina. Nat Neurosci. 2004; 7:745–750. [PubMed: 15208634]
12. Makous W, et al. Retinal microscotomas revealed with adaptive-optics microflashes. Invest Ophthalmol Vis Sci. 2006; 47:4160–4167. [PubMed: 16936137]
13. Wesner MF, Pokorny J, Shevell SK, Smith VC. Foveal cone detection statistics in color-normals and dichromats. Vision Res. 1991; 31:1021–1037. [PubMed: 1858318]
14. Reid RC, Shapley RM. Space and time maps of cone photoreceptor signals in macaque lateral geniculate nucleus. J Neurosci. 2002; 22:6158–6175. [PubMed: 12122075]
15. Johnson EN, Hawken MJ, Shapley R. Cone inputs in macaque primary visual cortex. J Neurophysiol. 2004; 91:2501–2514. [PubMed: 14749310]

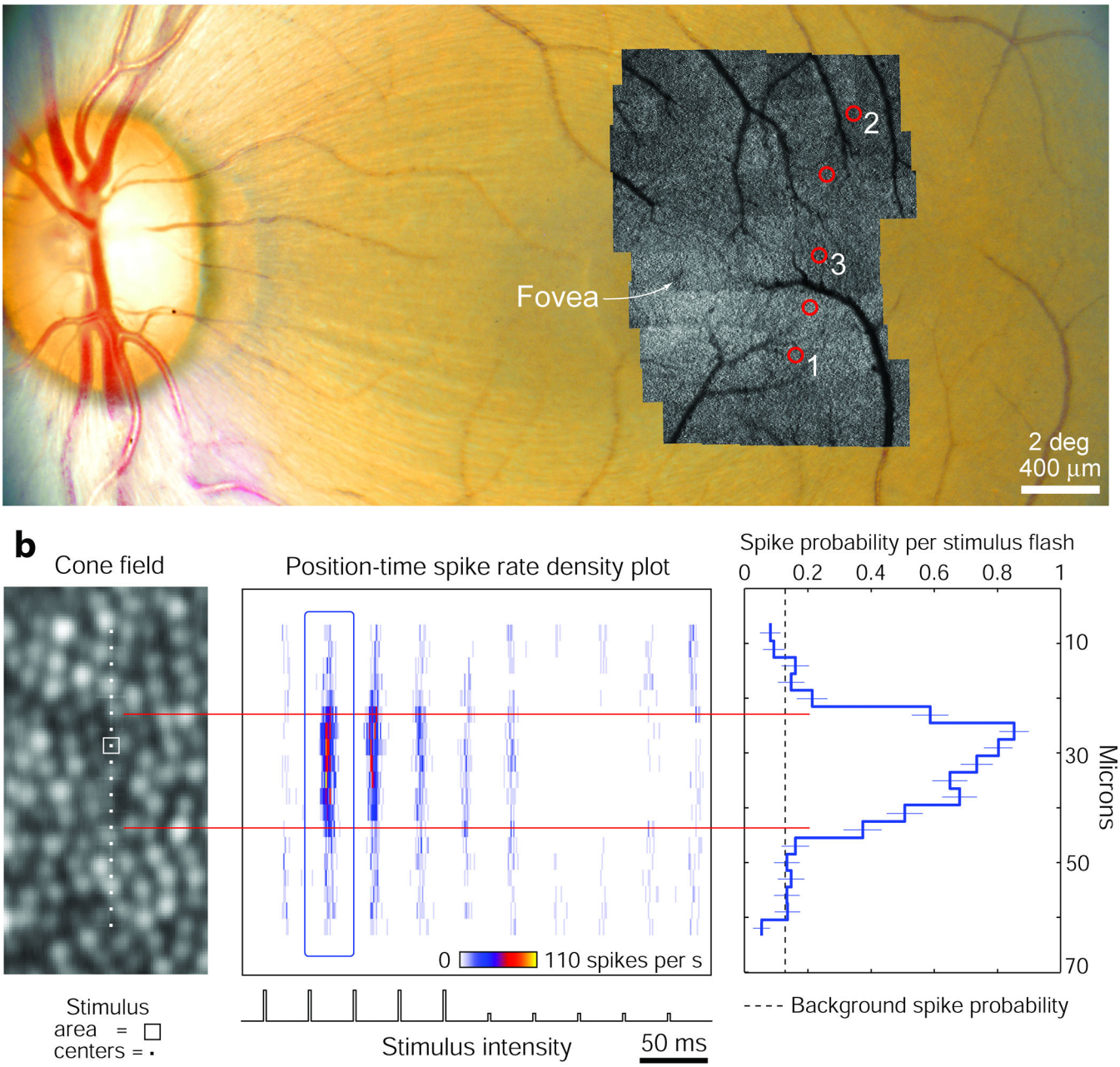

Figure 1. Localizing cone fields of LGN neurons

(**a**) Left eye fundus photograph with AOSLO images montaged over the macula where receptive fields (red circles) were recorded. Neurons analyzed in the figures are numbered for reference. (**b**) Stimuli flashed at 19 contiguous locations across the cone field of Neuron 1 (left) led to an adapting ON response and an inhibitory OFF response (middle, each row in the spike density plot represents the temporal response of one position in the cone field). Response latency was ~ 45 ms. Cone field is rotated 90° for display purposes. Residual light in the optical path generated background activity at the frame rate. Activity above the background rate occurred over a region spanning 4 cones, indicated by red lines. Mean spike

probability (right, ±1 s.e.m.) was measured in blue outlined area of the spike density plot. Micron scale applies to all panels.

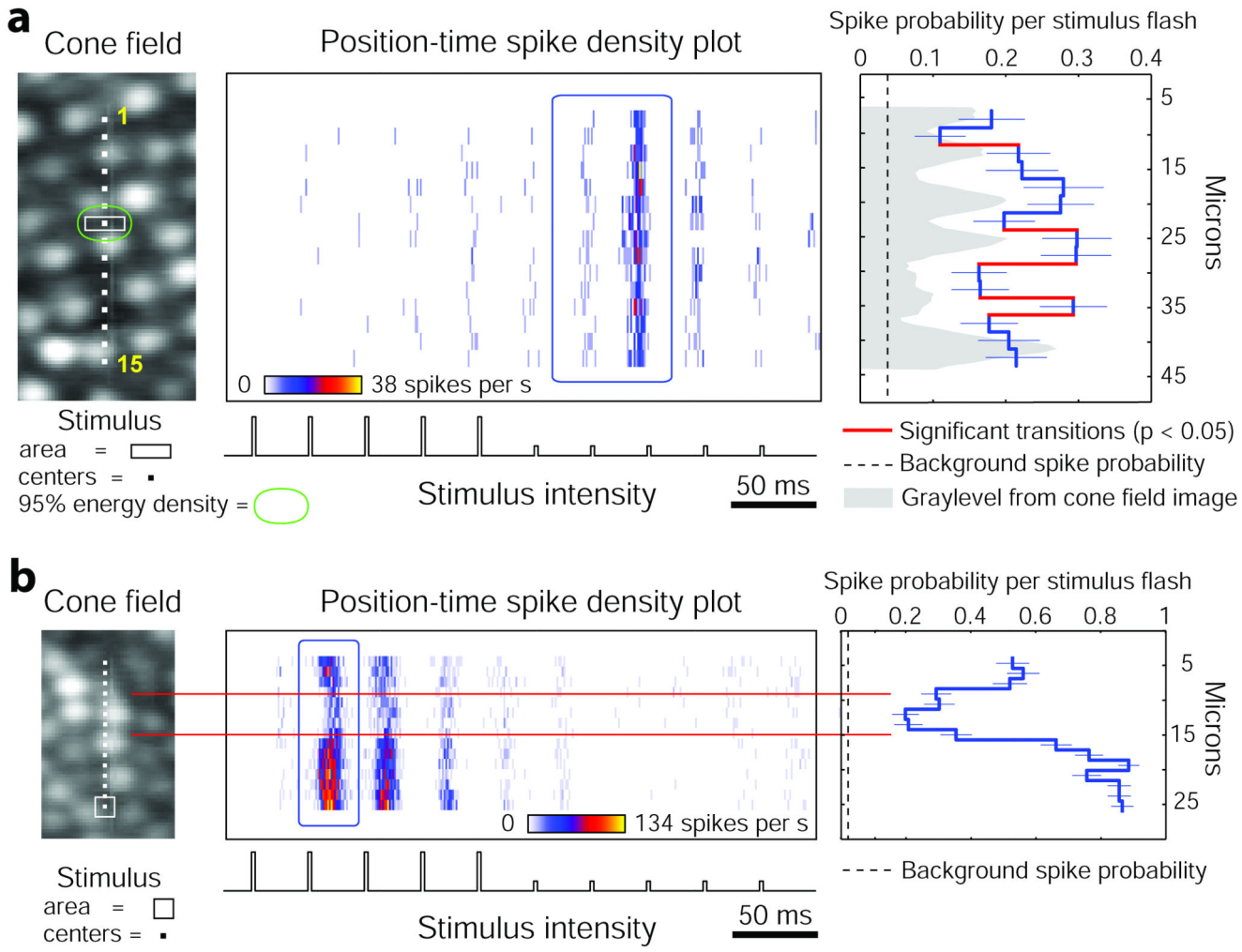

Figure 2. Parvocellular LGN activity varies with stimulus position and cone type

(**a**) Narrow 1.5 × 6 μm stimuli flashed at 15 positions resulted in OFF responses in Neuron 2 that were highest when stimuli landed on a cone (e.g. position 8), and significantly reduced when stimuli fell between cones (red transitions, one-tailed Fisher's exact test). The green contour shows the region where 95% of the time-averaged light energy was delivered for this stimulus, taking into account the point-spread function and motion remaining after stabilization. The targeted stimulus area (white) contained 66% of the delivered light. (**b**) Stimuli flashed at 15 overlapping positions yielded differential responses in Neuron 3 which depended on the cone being stimulated. The lowest response corresponded to one cone indicated between red lines. For all panels, mean probability per stimulus flash (±1 s.e.m.) was computed for blue outlined areas in the spike density plots. Micron scale applies to each row of panels.